Inorg. Chem. **2008**, *47*, 10841−10850

Theoretical Investigation of One- and Two-Photon Absorption Properties of Platinum Acetylide Chromophores

Zhao-Di Yang,[†,‡] Ji-Kang Feng,*[,†,§] and Ai-Min Ren[†]

State Key Laboratory of Theoretical and Computational Chemistry, Jilin University, Changchun 130023, China, Chemical and Environmental Engineering College, Harbin University of Science and Technology, Harbin 150040, China, and The College of Chemistry, Jilin University, Changchun 130023, China

Received March 7, 2008

In this paper, we have theoretically investigated bis((4-phenylethynyl)phenyl) ethynyl)bis(trimethylphosphine)platinum(II) (**PE2**) and its analogs—three platinum acetylide complexes (**1**−**3**) that feature highly π-conjugated ligands (alkynyl-dimethylfluorene substituted with electron-donating or -withdrawing moieties). The geometrical and electronic structures are calculated at the ECP60MWB//6-31G*(H, C, P, N, S) basis set level by the density functional theory (DFT) method; one-photon absorption properties have been calculated by using time-dependent DFT (TDDFT) and Zerner's intermediate neglect of differential overlap (ZINDO) methods, and two-photon absorption (TPA) properties are obtained with the ZINDO/sum-over-states method. The values of β_{sp} and β_{d} for Pt are adjusted to −1 eV and −28.5 eV, respectively, to make one-photon absorption spectra calculated by ZINDO closest to the experimental data and TDDFT results. The calculated results indicate that all molecules in this work (involving cis isomers of molecules **1**−**3**) take on two TPA peaks in the 600−800 nm region. The peak at 700−750 nm should not be simply attributed to the appearance of noncentrosymmetric cis isomers in solution, although trans and cis isomers adhere to a different selection rule. Every TPA peak results from its transition character. Molecules **1**−**3** show greater two-photon absorption strength compared with **PE2** and retain good transparency.

1. Introduction

Interest in two-photon absorbing materials has increased within the past decade because of their usefulness in various applications. They are being developed for use in 3D microfabrication,[1] photodynamic therapy,[2] two-photon microscopy,[3] optical power limiting (OPL),[4] optical data storage,[5] and two-photon laser scanning fluorescence imaging.[6] Many experimental and theoretical investigations have been done for seeking good two-photon absorption (TPA) materials with a big two-photon absorption cross-section at the wavelength of available laser sources.[7] Recently, organometallic compounds have become intriguing candidates of researchers as nonlinear optical (NLO) materials,[8] because (1) these compounds

* Author to whom correspondence should be addressed. Fax: (+86)431-88498026. E-mail: Jikangf@yahoo.com.
† State Key Laboratory of Theoretical and Computational Chemistry, Jilin University.
‡ Harbin University of Science and Technology.
§ The College of Chemistry, Jilin University.

(1) (a) Zhou, W.; Kuebler, S. M.; Braun, K. L.; Yu, T.; Cammack, J. K.; Ober, C. K.; Perry, J. W.; Marder, S. R. *Science* **2002**, *296*, 1106. (b) Kawata, S.; Sun, H.-B.; Tanaka, T.; Takada, K. *Nature* **2001**, *412*, 697. (c) Sun, H.-B.; Mizeikis, V.; Xu, Y.; Juodkazis, S.; Ye, J.-Y.; Matsuo, S.; Misawa, H. *Appl. Phys. Lett.* **2001**, *79*, 1. (d) Maruo, S.; Nakamura, O.; Kawata, S. *Opt. Lett.* **1997**, *22*, 132.
(2) Denk, W.; Strickler, J. H.; Webb, W. W. *Science* **1990**, *248*, 73.
(3) (a) Bhawalkar, J. D.; Kumar, N. D.; Zhao, C. F.; Prasad, P. N. *J. Clin. Laser Med. Surg.* **1997**, *15*, 201. (b) He, G. S.; Markowicz, P. P.; Line, P.-C.; Prasad, P. N. *Nature* **1999**, *415*, 767. (c) Xu, C.; Zipfel, W.; Shear, J. B.; Williams, R. M.; Webb, W. W. *Proc Natl. Acad. Sci. U.S.A.* **1996**, *93*, 10763. (d) Larson, D. R.; Zipfel, W. R.; Williams, R. M.; Clark, S. W.; Bruchez, M. P.; Wise, F. W.; Webb, W. W. *Science* **2003**, *300*, 1434.
(4) (a) He, G. S.; Xu, G. C.; Prasad, P. N.; Reinhardt, B. A.; Bhatt, J. C.; McKellar, R.; Dillard, A. G. *Opt. Lett.* **1995**, *20*, 435. (b) Calvete, M.; Yang, G. Y.; Hanack, M. *Synth. Met.* **2004**, *141*, 231.
(5) (a) Parthenopoulos, D. A.; Rentzepis, P. M. *Science* **1989**, *245*, 843. (b) Strickler, J. H.; Webb, W. W. *Opt. Lett.* **1991**, *16*, 1780. (c) Belfield, K. D.; Schafer, K. J. *Chem. Mater.* **2002**, *14*, 3656.
(6) Köler, R. H.; Cao, J.; Zipfel, W. R.; Webb, W. W.; Hanson, M. R. *Science* **1997**, *276*, 2039.
(7) (a) Albota, M.; Beljonne, D.; Brédas, J. L.; Ehrlich, J. E.; Fu, J.; Heikal, A. A.; Hess, E.; Kogej, T.; Levin, M. D.; Marder, S. R.; McCord-Maughon, D.; Perry, J. W.; Röeckel, H.; Rumi, M.; Subramaniam, G.; Webb, W. W.; Wu, X.; Xu, C. *Science* **1998**, *281*, 1653. (b) Yang, Z.-D.; Feng, J.-K.; Ren, A.-M. *J. Phys. Chem. A* **2006**, *110*, 13956. (c) Zhou, X.; Feng, J.-K.; Ren, A.-M. *Chem. Phys. Lett.* **2004**, *397*, 500.

10.1021/ic800417g CCC: $40.75
Published on Web 11/01/2008

can have metal-to-ligand (MLCT) or ligand-to-metal (LMCT) charge-transfer bands, which are often associated with larger optical nonlinearities, in the UV−visible region of the spectrum and (2) coordinating a ligand containing highly polarizable π electrons to a metallic center having weakly bound valence electrons could yield electronic structures that exhibit enhanced optical nonlinearities. Organometallic platinum compounds show large NLO effects and have promising OPL properties.[9] An interesting class of conjugated organometallic molecules is the platinum(II) alkynyl complexes, reported by Sonogashira and co-workers.[10] Pt acetylides generally have high linear transmission in most parts of the visible region and significant nonlinear absorption over a wide spectral region and are therefore particularly suitable for OPL applications. In the literature, there are several examples of Pt acetylides that exhibit TPA in the visible or near-IR region. In particular, bis((4-phenylethynyl)phenyl)ethynyl)bis(tributylphosphine) platinum(II) (simplified as **PE2**) has been widely studied for its OPL properties in many experimental studies, and it has a measurable intrinsic (femtosecond) two-photon absorption cross-section (δ) of 7 GM at 720 nm and 235 GM at 595 nm.[9c,e,11] The latter measurement was made using picosecond pulses, which allows for considerable excited-state absorption from both the S_1 and the T_1 excited states. This would correctly be termed an effective TPA cross-section. More recently, a dendron-decorated **PE2** series has been studied experimentally and was shown to have similar intrinsic δ values at 720 nm.[12] Platinum acetylides substituted with thiophene groups in place of phenyl groups have also shown a doubling of the intrinsic δ value at 740 nm.[13] The analogs of **PE2**, the platinum(II) complexes that carry two alkynyl-benzothiazolylfluorene ligands and two alkynyl- diphenylaminofluorene ligands, were synthesized and studied experimentally as two-photon chromphores.[14] Compared with **PE2**, these two platinum acetylides show greater two-photon absorption strength. However, the theoretical investigations about two-photon absorption properties of platinum acetylides are infrequent because there is a lack of default resonance integral parameters of the metal Pt atom, which are used to calculate the two-photon absorption properties in Zerner's intermediate neglect of differential overlap (ZINDO) method. Therefore, in this work, we will try to adjust and get a set of reasonable resonance integral parameters of metal Pt; then, the equilibrium geometries, the electronic structures, and one-photon absorption (OPA) and TPA properties of molecules **PE2**, **1** (platinum(II) complex that carries two alkynyl-diphenylaminofluorene ligands), **2** (platinum(II) complex that carries two alkynyl- benzothiazolylfluorene ligands), and **3** (platinum(II) complex that carries two alkynyl-diphenylaminophenylethynylfluorene ligands) will be studied in detail. In this work, the alkyls in the phosphorus atom and nine-position of fluorene are all replaced by methyl in order to simplify calculation.

2. Methods

2.1. Two-Photon Absorption. The TPA process corresponds to the simultaneous absorption of two photons. The TPA efficiency of an organic molecule, at optical frequency $\omega/2\pi$, can be characterized by the TPA cross-section $\delta(\omega)$. It can be directly related to the imaginary part of the third-order polarizability $\gamma(-\omega;\omega,\omega,-\omega)$,[15,16] as shown in eq 1:

$$\delta(\omega) = \frac{3\hbar\omega^2}{2n^2c^2\varepsilon_0} L^4 \mathrm{Im}\, \gamma(-\omega;\omega,\omega,-\omega) \qquad (1)$$

where $\gamma(-\omega;\omega,\omega,-\omega)$ is the third-order polarizability, $\hbar\omega$ is the energy of incoming photons, c is the speed of light, ε_0 is the vacuum electric permittivity, n denotes the refractive index of the medium, and L corresponds to the local-field factor. In the calculations presented here, n and L are set to 1 because of isolated molecules in the vacuum.

The sum-over-states (SOS) expression to evaluate the components of the second hyperpolarizability, $\gamma_{\alpha\beta\gamma\delta}$, can be educed using perturbation theory. By considering a Taylor expansion of energy with respect to the applied field, the $\gamma_{\alpha\beta\gamma\delta}$ Cartesian components are given by refs 17 and 18.

(8) (a) Liu, X.-J.; Feng, J.-K.; Ren, A. M.; Cheng, H.; Zhou, X. *J. Chem. Phys.* **2004**, *120*, 11493. (b) Sénéchal, K.; Maury, O.; Bozec, H. L.; Ledoux, I.; Zyss, J. *J. Am. Chem. Soc.* **2002**, *124*, 4560. (c) Das, S.; Nag, A.; Goswami, D.; Bharadwaj, P. K. *J. Am. Chem. Soc.* **2006**, *128*, 402. (d) Zhang, X.-B.; Feng, J.-K.; Ren, A.-M.; Sun, C.-C. *J. Phys. Chem. A* **2006**, *110*, 12222. (e) Zhang, X.-B.; Feng, J.-K.; Ren, A.-M. *J. Phys. Chem. A* **2007**, *111*, 1328.

(9) (a) McKay, T. J.; Bolger, J. A.; Staromlynska, J.; Davy, J. R. *J. Chem. Phys.* **1998**, *108* (13), 5537. (b) McKay, T. J.; Staromlynska, J.; Davy, J. R.; Bolger, J. A. *J. Opt. Soc. Am. B* **2001**, *18*, 358. (c) McKay, T. J.; Staromlynska, J.; Wilson, P.; Davy, J. R. *Appl. Phys.* **1999**, *85*, 1337. (d) Staromlynska, J.; Chapple, P. B.; Davy, J. R.; McKay, T. J. *Proc. SPIE* **1994**, *2229*, 59. (e) Staromlynska, J.; McKay, T. J.; Bolger, J. A.; Davy, J. R. *J. Opt. Soc. Am. B* **1998**, *15* (6), 1731. (f) Staromlynska, J.; McKay, T. J.; Wilson, P. *J. Appl. Phys.* **2000**, *88* (4), 1726. (g) Vestberg, R.; Malmstrøm, E.; Eriksson, A.; Lopes, C.; Lindgren, M. *Proc. SPIE* **2004**, *5621*, 31.

(10) (a) Sonogashira, K.; Fujikura, Y.; Yatake, T.; Toyoshima, N.; Takahashi, S.; Hagihara, N. *J. Organomet. Chem.* **1978**, *145*, 101. (b) Hagihara, N.; Sonogashira, K.; Takahashi, S. *Adv. Polym. Sci.* **1981**, *41*, 149.

(11) Glimsdal, E.; Eriksson, A.; Vestberg, R.; Malmstrom, E.; Lindgren, M. *SPIE Proc.* **2005**, *5934*, 1.

(12) Vestberg, R.; Westlund, R.; Ericksson, A.; Lopes, C.; Carlsson, M.; Eliasson, B.; Glimsdal, E.; Lindgren, M.; Malmstrom, E. *Macromolecules* **2006**, *39*, 2238.

(13) Glimsdal, E.; Carlsson, M.; Eliasson, B.; Minaev, B.; Lindgren, M. *J. Phys. Chem. A* **2007**, *111*, 244.

(14) Rogers, J. E.; Slagle, J. E.; Krein, D. M.; Burke, A. R.; Hall, B. C.; Fratini, A.; McLean, D. G.; Fleitz, P. A.; Cooper, T. M.; Drobizhev, M.; Makarov, N. S.; Rebane, A.; Kim, K.-Y.; Farley, R.; Schanze, K. S. *Inorg. Chem.* **2007**, *46*, 6483.

(15) Cha, M.; Torruellas, W. E.; Stegeman, G. I.; Horsthuis, W. H. G.; Möhlmann, G. R. *J. Methods Appl. Phys. Lett.* **1994**, *65*, 2648.

(16) Kogej, T.; Beljonne, D.; Meyers, F.; Perry, J. W.; Marder, S. R.; Brédas, J.-L. *Chem. Phys. Lett.* **1998**, *298*, 1.

(17) Orr, B. J.; Ward, J. F. *Mol. Phys.* **1971**, *20*, 513.

(18) Bishop, D. M.; Luis, J. M.; Kirtman, B. *J. Chem. Phys.* **2002**, *116*, 9729.

$$\gamma_{\alpha\beta\gamma\delta}(-\omega_\sigma;\omega_1,\omega_2,\omega_3) =$$

$$\hbar^{-3}\sum P_{1,2,3}\Bigg(\sum_K{}'\sum_L{}'\sum_M{}'\times$$

$$\Bigg(\frac{\langle 0|\mu_\alpha|K\rangle\langle K|\bar{\mu}_\beta|L\rangle\langle L|\bar{\mu}_\gamma|M\rangle\langle M|\mu_\delta|0\rangle}{(\omega_K - i\Gamma_K/2 - \omega_\sigma)(\omega_L - i\Gamma_L/2 - \omega_2 - \omega_3)(\omega_M - i\Gamma_M/2 - \omega_3)} +$$

$$\frac{\langle 0|\mu_\beta|K\rangle\langle K|\bar{\mu}_\alpha|L\rangle\langle L|\bar{\mu}_\gamma|M\rangle\langle M|\mu_\delta|0\rangle}{(\omega_K + i\Gamma_K/2 + \omega_1)(\omega_L - i\Gamma_L/2 - \omega_2 - \omega_3)(\omega_M - i\Gamma_M/2 - \omega_3)} +$$

$$\frac{\langle 0|\mu_\beta|K\rangle\langle K|\bar{\mu}_\gamma|L\rangle\langle L|\bar{\mu}_\alpha|M\rangle\langle M|\mu_\delta|0\rangle}{(\omega_K + i\Gamma_K/2 + \omega_1)(\omega_L + i\Gamma_L/2 + \omega_2 + \omega_3)(\omega_M - i\Gamma_M/2 - \omega_3)} +$$

$$\frac{\langle 0|\mu_\beta|K\rangle\langle K|\bar{\mu}_\gamma|L\rangle\langle L|\bar{\mu}_\delta|M\rangle\langle M|\mu_\alpha|0\rangle}{(\omega_K + i\Gamma_K/2 + \omega_1)(\omega_L + i\Gamma_L/2 + \omega_2 + \omega_3)(\omega_M + i\Gamma_M/2 + \omega_3)}\Bigg)$$

$$-\sum_K{}'\sum_L{}'\times$$

$$\Bigg(\frac{\langle 0|\mu_\alpha|K\rangle\langle K|\mu_\beta|0\rangle\langle 0|\mu_\gamma|L\rangle\langle L|\mu_\delta|0\rangle}{(\omega_K + i\Gamma_K/2 - \omega_\sigma)(\omega_K + i\Gamma_K/2 - \omega_1)(\omega_L + i\Gamma_L/2 - \omega_3)} +$$

$$\frac{\langle 0|\mu_\alpha|K\rangle\langle K|\mu_\beta|0\rangle\langle 0|\mu_\gamma|L\rangle\langle L|\mu_\delta|0\rangle}{(\omega_K - i\Gamma_K/2 - \omega_1)(\omega_L + i\Gamma_L/2 + \omega_2)(\omega_L - i\Gamma_L/2 - \omega_3)} +$$

$$\frac{\langle 0|\mu_\beta|K\rangle\langle K|\mu_\alpha|0\rangle\langle 0|\mu_\gamma|L\rangle\langle L|\mu_\delta|0\rangle}{(\omega_K + i\Gamma_K/2 + \omega_1)(\omega_K + i\Gamma_K/2 + \omega_\sigma)(\omega_L + i\Gamma_L/2 + \omega_2)} +$$

$$\frac{\langle 0|\mu_\beta|K\rangle\langle K|\mu_\alpha|0\rangle\langle 0|\mu_\gamma|L\rangle\langle L|\mu_\delta|0\rangle}{(\omega_K + i\Gamma_K/2 + \omega_1)(\omega_L + i\Gamma_L/2 + \omega_2)(\omega_L - i\Gamma_L/2 - \omega_3)}\Bigg)\Bigg) \quad (2)$$

In the formula α, β, γ, and δ refer to the molecular axes; ω_1, ω_2, and ω_3 are optical frequencies; and $\omega_\sigma = \omega_1 + \omega_2 + \omega_3$ is the polarization response frequency; $\sum P_{1,2,3}$ indicates a sum over the terms obtained by the six permutations of the pairs (ω_1/μ_β), (ω_2/μ_γ), and (ω_3/μ_δ); K, L, and M denote excited states, and 0 denotes the ground state; $|K\rangle$ is an electronic wave function with energy $\hbar\omega_K$ relative to the ground electronic state; μ_α is the αth ($= x, y, z$) component of the dipole operator, $\langle K|\bar{\mu}_\alpha|L\rangle = \langle K|\mu_\alpha|L\rangle - \langle 0|\mu_\alpha|0\rangle\delta_{KL}$; the primes on the summation over the electronic states indicate exclusion of the ground state. Γ_K is the damping factor of excited state K, and in the present work, all damping factors Γ are set to 0.14 eV; this choice of damping factor is found to be reasonable on the basis of the comparison between the theoretically calculated and experimental TPA spectra.[7] To compare the calculated δ value with the experimental value measured in solution, the orientationally averaged (isotropic) value of γ is evaluated,[19] which is defined as

$$\langle\gamma\rangle = \frac{1}{15}\sum_{i,j}(\gamma_{iijj} + \gamma_{ijij} + \gamma_{ijji}) \quad i,j = x,y,z \quad (3)$$

When the imaginary part of the $\langle\gamma\rangle$ value is substituted into eq 1, $\delta(\omega)$, which can be compared with the experimental value, is obtained. We have compiled a program (FTRNLO) to calculate the second hyperpolarizability, γ, and the TPA cross-section, δ, according to formulas 1−3.

2.2. Quantum Chemical Calculations. In principle, any kind of self-consistent-field molecular orbital procedure combined with a configuration interaction (CI) can be used to calculate the physical values in the SOS expressions. In this paper, the ground-state equilibrium geometries of all molecules were optimized by using DFT/B3LYP calculations, which are remarkably successful in predicting a wide variety of problems in organometallic chemistry.[20] Gradient optimizations were carried out using the 6-31G* basis set[21] for C, P, S, N, and H atoms. Owing to the large number of electrons and to account for relativistic effects, the basis sets with inner electrons substituted by effective core potentials (ECP) were employed for Pt. The basis set employed for platinum is the ECP60MWB pseudopotential of the Stuttgart/Bonn group (where M indicates that the neutral atom is used in the derivation of the ECP and WB implies the use of the quasirelativistic approach described by Wood and Boring).[22] This yields the ECP60MWB (8s7p6d)/[(6s5p3d)]//6−31G*(H, C, P, N, S) basis set for platinum acetylide systems, denoted as E60.

Then, the properties of electronic excited states were obtained by single-electron excitation and double-electron excitation configuration interactions using the ZINDO program. For all of the molecules, the Mataga−Nishimoto potential was employed to describe long-range Coulomb interactions; the CI-active spaces were restricted to the 30 highest-occupied and 30 lowest-unoccupied π orbitals for the singly excited configuration and to the two highest-occupied and two lowest-unoccupied π orbitals for the doubly excited configuration. However, the implementation of ZINDO includes default values for numerous parameters. The resonance integrals for the central metal, β_s, β_p, and β_d in transition metal complexes are important parameters that can be commonly adjusted.[23] β_s and β_p are set equal ("β_{sp}") and represent the amount of interaction between s and p orbitals on the metal and those on adjacent ligand atoms. The β_d values represent interaction of the metal d orbitals with ligands. Values which are more negative represent a greater interaction between the corresponding metal orbital(s) and ligand orbitals. It is well-known that the ZINDO program does not include the default values of resonance integrals for metal Pt. But we know that β_{sp} and β_d in transition metal complexes can be commonly adjusted. Values of β_{sp} for Ni have ranged from −1 to −32 eV, and the values of β_d for Ni have ranged from −29 to −45 eV.[23] The values of β_{sp} and β_d parameters suitable for the single molecule could be determined by the closest agreement of the resulting calculated electronic absorption spectrum with experimental results. Therefore, we find that the values of β_{sp} and β_d for metal Pt are −1 and −28.5 eV, respectively, because these values can lead to calculated electronic absorption spectra of molecules **PE2**, **1**, and **2** by using ZINDO that are closest

(19) Beljonne, D.; Wenseleers, W.; Zojer, E.; Shuai, Z. G.; Vogel, H.; Pond, S. J. K.; Perry, J. W.; Marder, S. R.; Brédas, J.-L. *Adv. Funct. Mater.* **2002**, *12*, 631.

(20) (a) Ziegler, T. *Chem. Rev.* **1991**, *91*, 651. (b) Niu, S.; Hall, M. B. *Chem. Rev.* **2000**, *100*, 353. (c) Li, S.; Hall, M. B. *Organometallics* **2001**, *20*, 2153. (d) Conner, D.; Jayaprakash, K. N.; Cundari, T. R.; Gunnoe, T. B. *Organometallics* **2004**, *23*, 2724. (e) Urtel, H.; Bikzhanova, G. A.; Grotjahn, D. B.; Hofmann, P. *Organometallics* **2001**, *20*, 3938. (f) Iron, M. A.; Martin, J. M. L.; Van der Boom, M. E. *J. Am. Chem. Soc.* **2003**, *125*, 11702.

(21) Hariharan, P. C.; Pople, J. A. *Theor. Chim. Acta* **1973**, *28*, 213.

(22) Andrae, D.; Haeussermann, U.; Dolg, M.; Stoll, H.; Preuss, H. *Theor. Chim. Acta* **1990**, *77*, 123.

(23) (a) Anderson, W. P.; Edwards, W. D.; Zerner, M. C. *Inorg. Chem.* **1986**, *25*, 2728. (b) Mantz, Y. A.; Musselman, R. L. *Inorg. Chem.* **2002**, *41*, 5770. (c) Anderson, W. P.; Cundari, T. R.; Drago, R. S.; Zerner, M. C. *Inorg. Chem.* **1990**, *29*, 1.

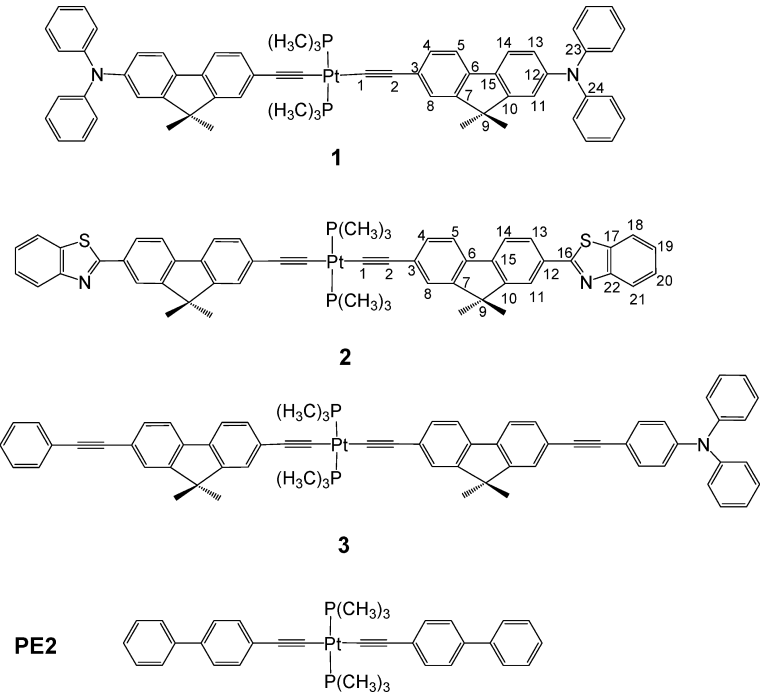

Figure 1. Investigated molecular structures and corresponding names and labels.

to the experimental UV−vis spectra. At the same time, the time-dependent density functional theory (TDDFT) method at the B3LYP level is also used to calculate the electronic absorption spectra in order to further confirm the rationality of the values of β_{sp} and β_{d} for metal Pt in ZINDO calculations.

3. Results and Discussions

3.1. Molecule Geometries. The structures of all investigated molecules and corresponding names and labels are displayed in Figure 1. The molecule **PE2** is usually considered to be a convenient benchmark because it has been studied rather extensively; therefore, in this work, it was also studied to carry out a comparative investigation. Compared with **PE2**, the ligands of molecules **1**, **2**, and **3** are nonsymmetrical, so there are at least two isomers for molecules **1**−**3** (trans isomers with *Ci* symmetry and cis isomers with no symmetrical limit). Both isomers are optimized in this work because the centrosymmetric molecules and the noncentrosymmetric ones have different selection rules for TPA. The optimized molecular equilibrium geometries at the B3LYP/E60 level and corresponding energies (a.u.) are shown in Figure 2. The geometric parameters of molecules **1-trans** and **2-trans** are listed in Table 1 in the Supporting Information. The calculated results show that the calculated bond lengths and bond angles of molecules **1-trans** and **2-trans** are in good agreement with the experimental results of X-ray diffraction,[14] which demonstrates that the selected basis set in gradient optimizations is appropriate. It is well-known that accurate calculation for ground-state geometries is the basis of accurate calculation of one- and two-photon absorption spectra. As shown in Figure 2, the optimized results show that platinum is square-coordinated in all investigated platinum acetylides, and two $-P(CH_3)_3$ ligands are in a trans arrangement (the bond angle P−Pt−P is 180°). The ligand planes (alkynyl−fluorene plane or alkynyl−benzene plane) are almost vertical to the Pt coordinated plane (as shown in Table 1 in the Supporting Information, the dihedral angles P−Pt−C3−C4 of molecules **1-trans** and **2-trans** are 84° and 80°, respectively). The molecule **2-para** is the isomer of **2-trans** and is optimized in order to compare its geometrical stability with that of **2-trans**. In **2-para**, alkynyl−fluorenes and the Pt coordinated plane are located in the same plane. The calculation shows that the energy of **2-trans** is lower by 0.038 eV than that of **2-para**, so the structures in which ligand planes are vertical to the Pt coordinated plane are more stable geometrical structures.

3.2. Electronic Structures and One-Photon Absorption. Electronic structures are fundamental for the interpretation and understanding of the absorption spectra. The calculated frontier orbital energy levels (four occupied and four unoccupied orbitals and energy gaps between the highest occupied molecular orbital (HOMO) and lowest unoccupied molecular orbital (LUMO) for molecules **1-trans**, **2-trans**, **3-trans**, and **PE2**) are shown in Figure 3. As shown in Figure 3, the energy gaps between the HOMO and LUMO of molecules **1-trans**, **2-trans**, and **3-trans** are all smaller than that of **PE2**. The order of energy gaps is **PE2** (3.73 eV) > **1-trans** (3.68 eV) > **2-trans** (3.32 eV) > **3-trans** (3.30 eV). From the view of molecular design, molecule **2** is formed when the electron-donating groups (diphenylamino) at the end of **1** are replaced by electron-withdrawing groups (benzothiazolyl) and **3** is formed when alkynyl-benzene is added between fluorene and diphenylamino; therefore, the energy gaps of **2-trans** and **3-trans** are smaller than that of **1-trans** because electron-withdrawing substituents increase the molecular delocalization and the addition of alkynyl-

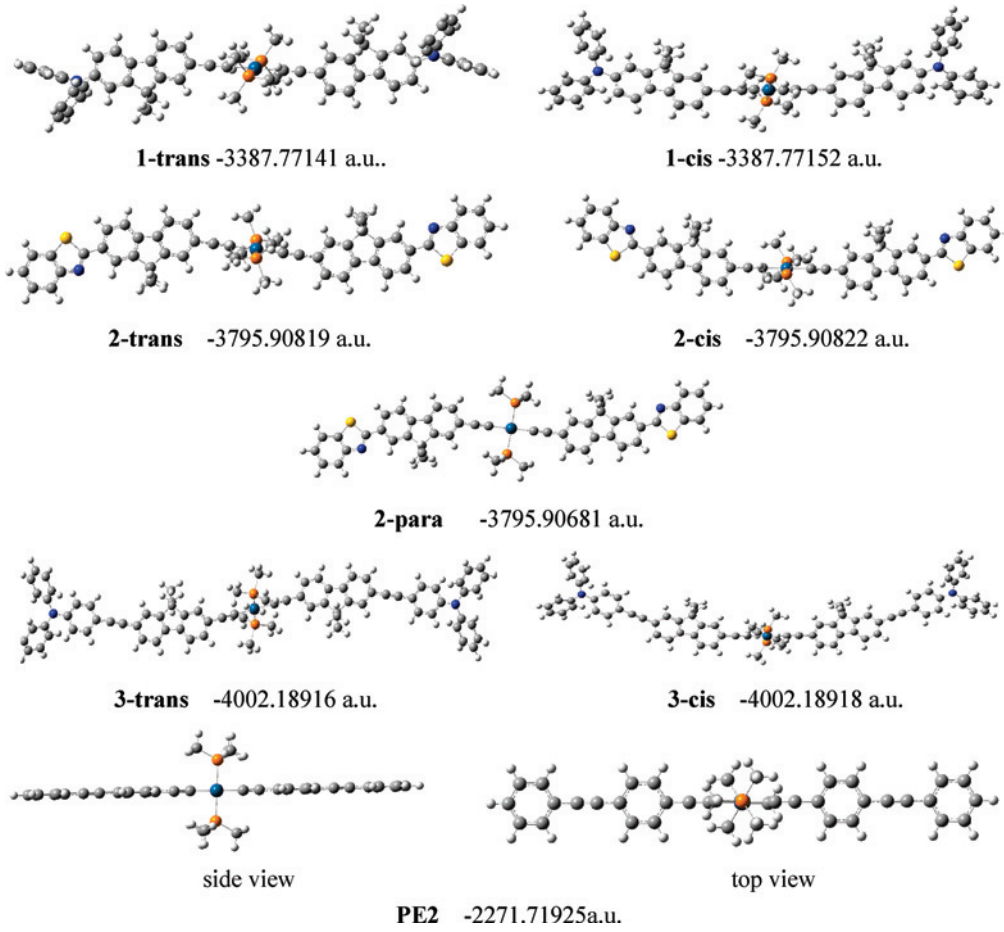

Figure 2. Calculated ground-state geometries for molecules **1**, **2**, **3**, and **PE2**.

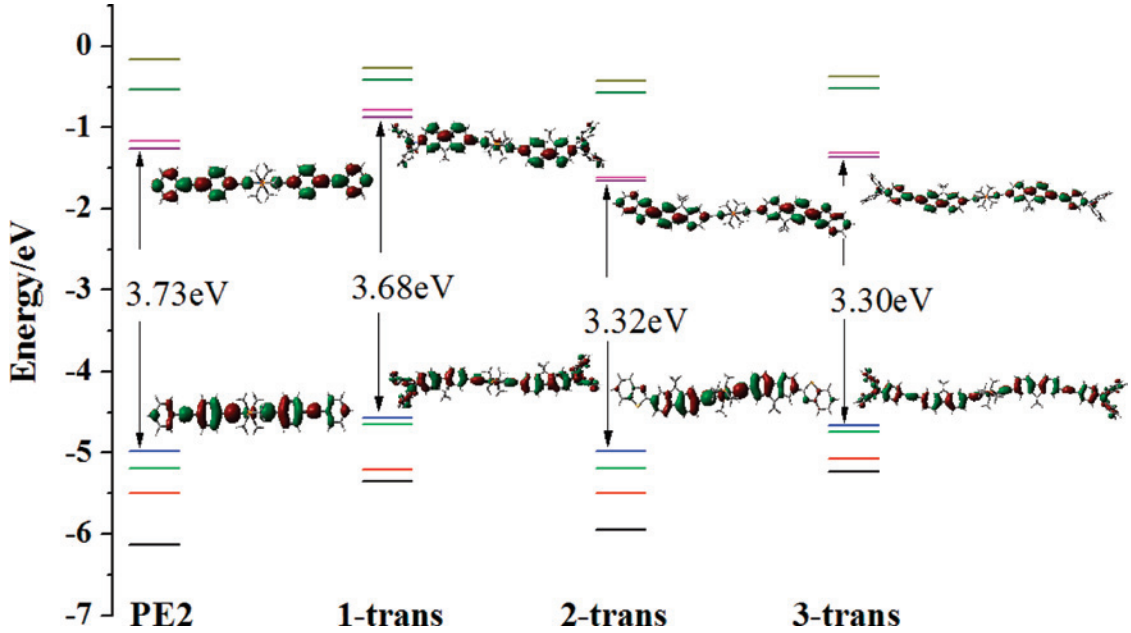

Figure 3. Calculated frontier orbitals' energy levels and the contour surfaces of HOMO and LUMO orbitals.

benzene results in the increase of conjugation. The contour surfaces of the HOMO and LUMO orbitals are also given in Figure 3 because the main configurations of maximal one-photon absorption states of all molecules are HOMO → LUMO. We can find from Figure 3 that the composition of the HOMO of every molecule is mainly bonding π orbitals in the ligands and d orbital of metal Pt; however, the composition of the LUMO is mainly antibonding π^* orbitals in the ligands without the contribution of the central Pt atom. So the character of the transition HOMO → LUMO of every molecule is primarily a $\pi-\pi^*$ transition with MLCT character.

Table 1. One-Photon Absorption Properties of All Molecules in the System

	ZINDO			TDDFT			
molecules	λ_{max}^{O}/nm	f^a	main configurations and weights[b]	λ_{max}^{O}/nm	f	main configurations and weights	exptl. data
PE2	378.0	2.67	−0.66(H → L)	363.8	2.67	0.66(H → L)	355, 357[24]
1-trans	379.5	2.44	0.53(H → L)	379.9	2.71	0.60(H → L)	383[14]
1-cis	379.7	2.39	0.53(H → L)	380.0	2.63	0.60(H → L)	
2-trans	391.9	3.39	−0.61(H → L)	412.9	2.59	0.65(H → L)	402[14]
2-cis	390.5	3.44	0.62(H → L)	411.6	2.53	0.65(H → L)	
3-trans	396.1	4.33	−0.59(H → L)	423.0	4.78	0.60(H → L)	
3-cis	395.7	4.04	−0.59(H → L)	422.4	4.40	0.58(H → L)	

[a] Note: f is the oscillator strength. [b] H denotes the HOMO and L denotes the LUMO.

Table 2. Two-Photon Absorption Properties

molecule	λ_{max}^{T}/nm	δ_{max}^{T}/GM	transition nature	main configurations and weights	character
PE2	715.4(720)[11−14]	137.9(7)[11−14]	$S_0 \rightarrow S_7$	−0.59(H−2 → L) − 0.64(H → L+1)	$\pi-\pi^*$, MLCT
	597.2(595)[9c,e]	192.4(235)[9c,e]	$S_0 \rightarrow S_{17}$	−0.36(H−4 → L) − 0.40(H−3 → L+1) +0.34(H−2 → L+6) − 0.43(H → L+9)	$\pi-\pi^*$, MLCT, LLCT
1-trans	715.4(720)[14]	34.0(140)[14]	$S_0 \rightarrow S_6$	−0.60(H−1 → L) − 0.63(H → L+1)	$\pi-\pi^*$, LLCT, LMCT
	602.8(612)[14]	405.2(780)[14]	$S_0 \rightarrow S_{20}$	−0.46(H−4 → L) + 0.51(H−3 → L+1)	LLCT, MLCT
1-cis	715.4	33.4	$S_0 \rightarrow S_6$	−0.60(H−1 → L) − 0.63(H → L+1)	$\pi-\pi^*$, LLCT, LMCT
	602.8	395.9	$S_0 \rightarrow S_{20}$	0.46(H−4 → L) − 0.51(H−3→L+1)	LLCT, MLCT
2-trans	738.6(720)[14]	171.9(370)[14]	$S_0 \rightarrow S_5$	−0.78(H → L+2)	LMCT
	640.8(649)[14]	265.5(415)[14]	$S_0 \rightarrow S_{14}$	0.34(H−2 → L+10) − 0.36(H−3 → L+11)	LLCT, MLCT
2-cis	738.4	167.1	$S_0 \rightarrow S_5$	−0.78(H → L+2)	LMCT
	640.8	258.6	$S_0 \rightarrow S_{14}$	0.34(H−2 → L+10) − 0.36(H−3 → L+11)	LLCT, MLCT
3-trans	742.8	49.2	$S_0 \rightarrow S_5$	0.36 (H−3 → L+2) + 0.85(H → L+2)	LMCT
	643.4	456.0	$S_0 \rightarrow S_{18}$	0.58(H−16 → L) − 0.59(H−15 → L+1)	LLCT
3-cis	742.4	49.8	$S_0 \rightarrow S_4$	0.35(H−3 → L+2) − 0.85(H → L+2)	LMCT
	643.4	429.9	$S_0 \rightarrow S_{18}$	0.52(H−16 → L) + 0.47(H−15 → L+1)	LLCT

OPA properties of all of the investigated molecules are calculated using the ZINDO program on the basis of optimized geometric structures. At the same time, for proving the veracity of the ZINDO method for calculating spectra, the TDDFT method was also adopted to calculate the OPA properties of all studied molecules. The maximal OPA wavelengths (λ_{max}^{O}), the corresponding oscillator strengths (f), and the main configurations and weights generated by the two methods are both listed in Table 1, and some experimental referenced data are given. Comparing the results calculated by TDDFT and ZINDO, we can find that the wavelength differences between them are small (average 16 nm). The maximal OPA wavelengths generated by the two methods are both in good agreement with the experimental observations, and the results given by the ZINDO method are closer to the experimental data. Table 1 also indicates that the oscillator strengths obtained by ZINDO are almost equal to those obtained by TDDFT, except for molecule **1**, and the main configurations and weights calculated by the two methods are in accordance with each other. Therefore, a semiempirical ZINDO method is appropriate for the studied molecules in this work, and the selection of resonance integral parameters is reasonable. A successful calculation for OPA properties by estimating and tuning the β_d value in the ZINDO program is very helpful for calculating two-photon absorption.

In succession, we compare the OPA properties of all molecules lengthways. As seen clearly in Table 1, the λ_{max}^{O} values of molecules **1**, **2**, and **3** are all red-shifted relative to **PE2**; the order of λ_{max}^{O} is **PE2** < **1** < **2** < **3**. Molecule **2**, with electron-withdrawing substituents (benzothiazolyl), has a longer OPA wavelength compared with molecule **1**, with electron-donating substituents (diphenylamino). The λ_{max}^{O} of molecule **3** is red-shifted relative to molecule **1** because molecule **3** has an added conjugation segment—alkynylbenzene. For molecules **1**, **2**, and **3**, one-photon absorption properties of their trans and cis isomers are both calculated, and the results clearly show that the trans isomers have almost the same maximal one-photon absorption wavelengths as the cis isomers, as shown in Table 1. In addition, the calculated λ_{max}^{O} values of the studied molecules are all located in the UV region, as shown in Table 1. This indicates that the investigated Pt-acetylides retain good transparency, which is important for OPL applications.

3.3. Two-Photon Absorption. The calculated TPA maximal absorption wavelength, λ_{max}^{T}; maximal TPA cross-section, δ_{max}^{T}; transition nature, and configurations and weights of the final states of TPA and their transition characters are collected in Table 2. In order to provide a clearer comparison for the molecules studied in this work, two-photon absorption spectra in the incident wavelength range of 600−800 nm are shown in Figure 4. As shown in Table 2, the calculated two-photon maximal absorption wavelengths (λ_{max}^{T}) are in good agreement with the experimental results (the differences are smaller than 10 nm); however, the calculated maximal two-photon absorption cross-sections (δ_{max}^{T}) are smaller than experimental observation values on the whole. For example, the two-photon absorption cross-section of **PE2** measured at 595 nm is a 235 GM (1 GM = 10^{-50}cm s/photon). This value was obtained with the z-scan technique using 27 ps pulses, which includes an excited-state absorption contribution,[9c,e,14] and

(24) (a) Cooper, T. M.; Krein, D. M.; Burke, A. R.; McLean, D. G.; Rogers, J. E.; Slagle, J. E.; Fleitz, P. A. *J. Phys. Chem. A* **2006**, *110*, 4369. (b) Rogers, J. E.; Hall, B. C.; Hufnagle, D. C.; Slagle, J. E.; Ault, A. P.; McLean, D. G.; Fleitz, P. A.; Cooper, T. M. *J. Chem. Phys.* **2005**, *122*, 214708.

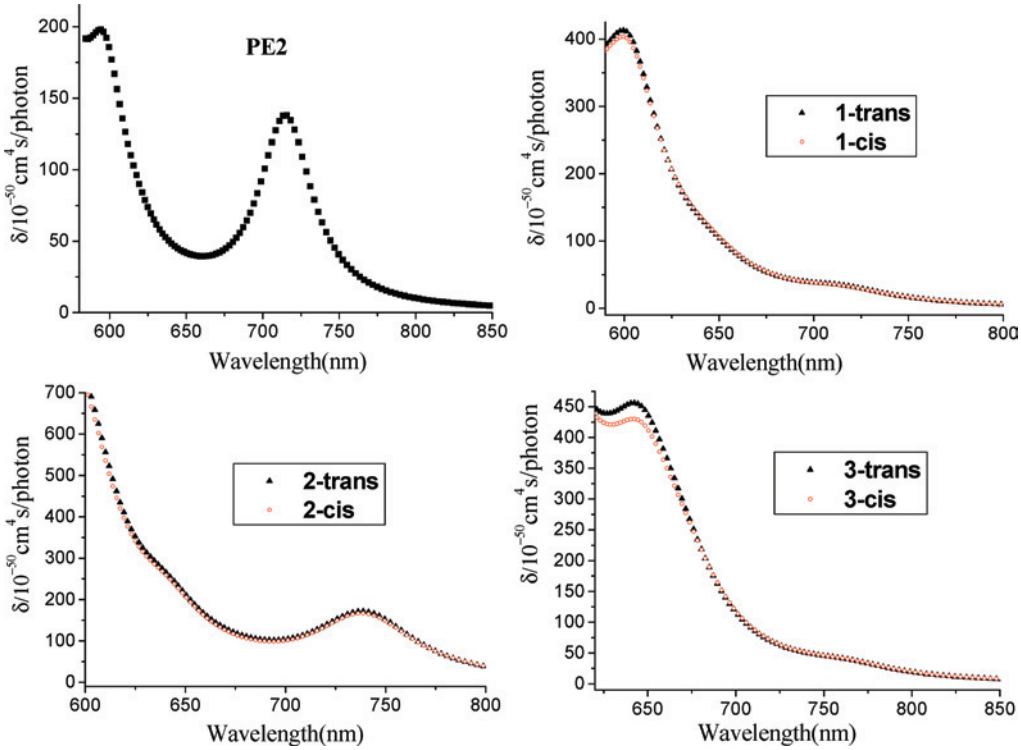

Figure 4. Two-photon absorption spectra.

Table 3. Channel Controlling the Third-Order Polarizability(γ) for All Studied Molecules

molecules	I$m\gamma$/10^{-34}esu	channel
PE2	4285.93	$S_0-S_3-S_7-S_3-S_0$
	4167.58	$S_0-S_3-S_{17}-S_3-S_0$
1-trans	1056.93	$S_0-S_2-S_6-S_2-S_0$
	8932.67	$S_0-S_2-S_{20}-S_2-S_0$; $S_0-S_4-S_{20}-S_4-S_0$; $S_0-S_5-S_{20}-S_5-S_0$
1-cis	1039.15	$S_0-S_2-S_6-S_2-S_0$
	8727.47	$S_0-S_2-S_{20}-S_2-S_0$; $S_0-S_4-S_{20}-S_4-S_0$; $S_0-S_5-S_{20}-S_5-S_0$
2-trans	5688.77	$S_0-S_2-S_4-S_2-S_0$; $S_0-S_2-S_5-S_2-S_0$
	6600.67	$S_0-S_2-S_{14}-S_2-S_0$
2-cis	5529.05	$S_0-S_2-S_4-S_2-S_0$; $S_0-S_2-S_5-S_2-S_0$
	6431.00	$S_0-S_2-S_{14}-S_2-S_0$
3-trans	1641.64	$S_0-S_2-S_5-S_2-S_0$
	11411.2	$S_0-S_2-S_{17}-S_2-S_0$; $S_0-S_2-S_{18}-S_2-S_0$; $S_0-S_2-S_{20}-S_2-S_0$
3-cis	1659.82	$S_0-S_2-S_4-S_2-S_0$
	10756.3	$S_0-S_2-S_{17}-S_2-S_0$; $S_0-S_2-S_{18}-S_2-S_0$; $S_0-S_2-S_{20}-S_2-S_0$

thus $\delta = 235$ GM can be considered as an upper limit for the intrinsic TPA cross-section. However, for molecules **1** and **2**, the experimental data were measured using the sample fluorescence relative to a bis-diphenylaminostilbene solution in methylene chloride. Therefore, although the calculated TPA cross-sections are smaller on the whole compared with experimental data, it does not affect our comparative investigation because the magnitude and law of comparison are not changed. From Table 2 and Figure 4, one can find that four compounds (**PE2**, **1**, **2**, and **3**) show a similar behavior. There are two TPA peaks in the range 600−800 nm (one is around 700−800 nm and has a moderately strong TPA transition, and the other is in the range 600−650 nm and has a very strong TPA), which is in good accordance with experimental results in ref 14.

In the literature,[14] researchers think the strong TPA peak experimentally observed in the region 600−700 nm is not reproduced in the one-photon absorption (there are no isolated peaks at 300−350 nm in OPA) and that this TPA peak can be tentatively assigned to a one-photon-forbidden, but two-photon-allowed, gerade−gerade transition; however, in solution, there are at least two different isomers, one of them being centrosymmetric, while the others are not. Therefore, the researchers thought the TPA peaks in the 700−800 nm region for molecules **1**, **2**, and **3** were attributed to the presence of noncentrosymmetric isomers. For validating this opinion, the TPA properties of both trans (centrosymmetric) and cis isomers (noncentrosymmetric) are calculated, and the results are shown in Table 2.

It is well-known that one- and two-photon absorptions adhere to different selection rules. For the molecule that has central symmetry, a change in the parity between the initial and final states (wave functions) is required for every photon involved in the transition for electric dipole transitions. Thus, the selection rule for TPA is different from that of OPA. One change of parity is required for a one-photon transition, while two-photon transitions must have initial and final states with the same parity. But noncentrosymmetric molecules adhere to the same selection rules for OPA and TPA. According to the above rules, for every molecule (whether it is a trans or cis isomer), we selected several excited states of two-photon absorption allowed as the two-photon absorption final states and calculated the two-photon absorption cross sections, δ, and then we obtained the maximal δ_{max}

and corresponding λ_{max} for every molecule. The results show that our calculations do not give the same conclusion that the authors came to in ref 14. As shown in Table 2 and Figure 4, both trans and cis isomers of molecules **1**, **2**, and **3** have two TPA peaks in the 600−700 (stronger) and 700−800 (weaker) ranges, respectively. For every TPA peak, the λ_{max}^{T} value of the trans isomer is almost equal to that of the cis isomer, and the difference of δ_{max}^{T} between the trans and cis isomers is very little. At the same time, the final states of TPA and the main configurations and charge transfer characters are also the same for both isomers. In order to further explain the calculated results, we provide ZINDO predicted transition dipole moments between main electronic states and the channel that controls the third-order polariz-

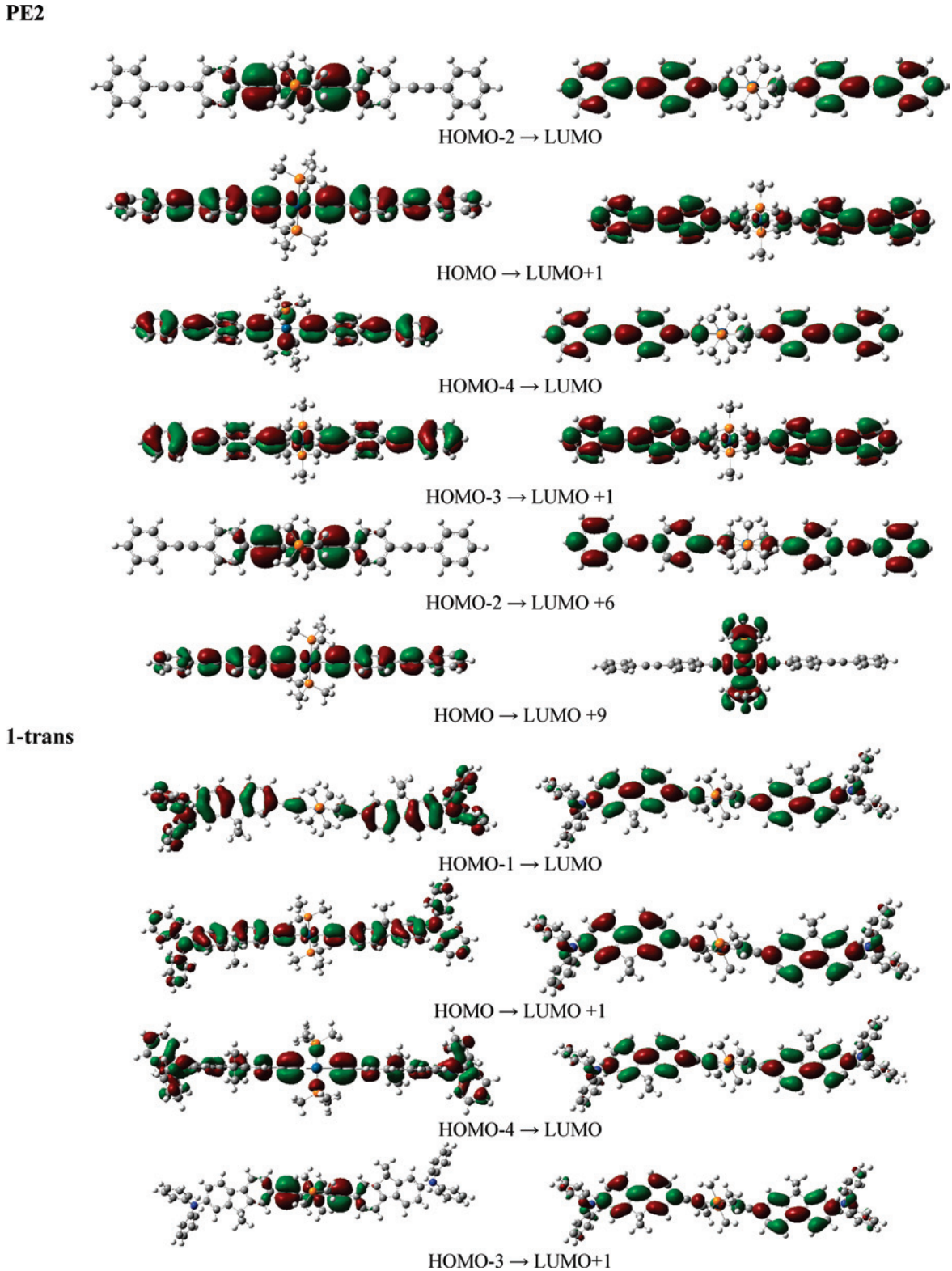

Figure 5

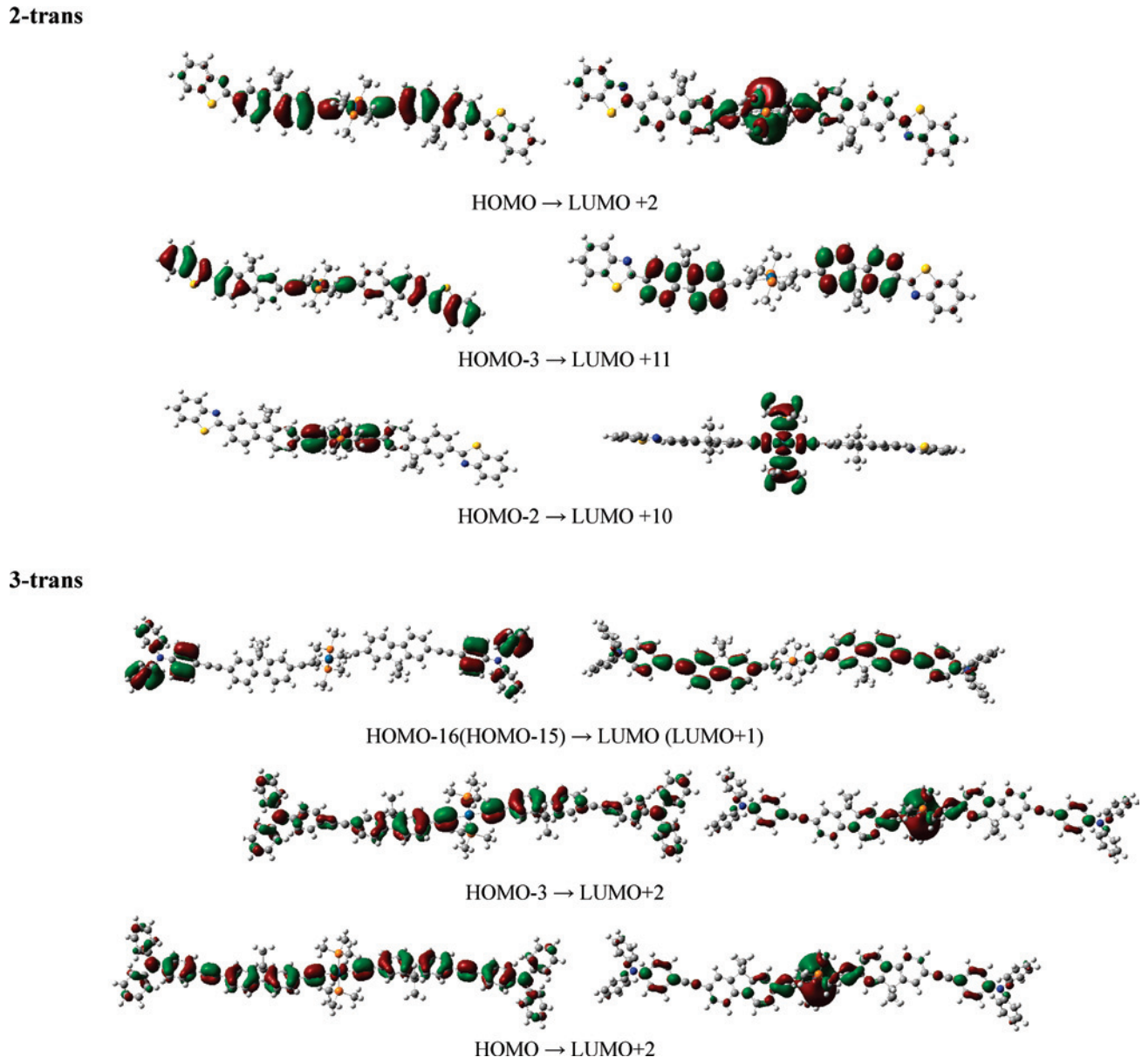

Figure 5. Contour surfaces of the frontier orbitals relevant to the maximal two-photon absorptions for **PE2**, **1-trans**, **2-trans**, and **3-trans**.

ability (γ) of all studied molecules (see Figure 2 in the Supporting Information and Table 3 in the text). One can find that the number of excited states for which two-photon absorption is allowed for trans isomers is less than that for cis isomers, according to the selective rules, but the crucial excited states with a larger transition dipole moment are the same compared with the cis ones. That is, the added states of cis isomers take on a smaller transition dipole moment and cannot influence the selection of middle and final states of maximal two-photon absorption. Therefore, both isomers have equal channels that control the third-order polarizability (γ) resulting in the same transition nature and same CI coefficients as shown in Table 3.

On the basis of the above discussions, we know that the weaker TPA peak in 700−800 nm for the molecules **1**, **2** and **3** should not be simply attribute to the presence of noncentrosymmetric isomers in solution according to the selection rules. For every molecule, the simultaneous presence of two TPA peaks may result from different transition characters. Figure 5 gives the contour surfaces of the frontier orbitals relevant to the maximal two-photon absorptions for **PE2**, **1-trans**, **2-trans**, and **3-trans**. As shown in Figure 5 and Table 2, the stronger TPA (at 597.2 nm) of **PE2** comes from electronic excitation $S_0 \rightarrow S_{17}$, which can be described as a linear addition of configurations HOMO−4 → LUMO, HOMO−3 → LUMO+1, HOMO−2 → LUMO+6, and HOMO → LUMO+9. The transition character is primarily a $\pi-\pi^*$ transition with MLCT and LLCT transition. The weaker TPA (at 715.4 nm) of **PE2** comes from $S_0 \rightarrow S_7$. The linear addition of configurations of S_7 is −0.59 (HOMO−2 → LUMO)−0.64 (HOMO → LUMO+1), and the transition character is a $\pi-\pi^*$ transition with MLCT. Comparing **1-trans**, **2-trans**, and **3-trans** with **PE2**, in the 600−700 nm region, the maximal two-photon absorption

cross-sections (δ_{max}^{T}) of **1-trans**, **2-trans**, and **3-trans** are larger than that of **PE2**, and the values are increased gradually in the order **PE2** = 192.4 GM < **2-trans** = 265.5 GM < **1-trans** = 405.2 GM < **3-trans** = 456.0 GM; the maximal two-photon absorption wavelengths are red-shifted relative to **PE2**. Herein, the charge transfer characters of **1-trans** and **2-trans** are the same (belonging to LLCT and MLCT, as shown in Figure 5 and Table 2), and the charge transfer character of **3-trans** is only LLCT. Now, we concentrate on the weaker TPA band (in the range 700−750 nm). The maximal two-photon absorption cross-section of **2-trans** is larger than that of **PE2**, but the values of **1-trans** and **3-trans** are very small. The two-photon absorption final state of **2-trans** is S_5. Its main configuration is HOMO → LUMO+2, and the transition character is LMCT. The ends of the **1-trans** molecule are electron-donating substituents—diphenylamino groups—its maximal two-photon absorption wavelengths are blue-shifted relative to the molecule **2-trans**, with benzothiazolyl groups at the end because the two-photon absorption final state of **1-trans** is the higher exited state S_6, whose transition character is a $\pi-\pi^*$ transition with LMCT and LLCT. The molecule **3-trans** is formed by increasing a conjugated segment (alkynyl-benzene) in comparison with **1-trans**, which leads to a red shift of TPA spectra and an increase of two-photon absorption cross-sections, as shown in Table 2.

4. Conclusion

Systematic theoretical investigations of the electronic structures and OPA and TPA properties have been completed for platinum acetylides **PE2**, **1**, **2**, and **3**. We have obtained a set of resonance integral parameters for the first time by tuning them up to make OPA results calculated by ZINDO/CI closer to the experimental data and TDDFT calculations. On the basis of the accurate calculation of molecular geometries and OPA spectra, the TPA properties are discussed in detail. There are two TPA peaks for every molecule in the range of 600−800 nm. The peak at 700−750 nm is not simply attributable to the appearance of noncentrosymmetric isomers in solution; the simultaneous presence of two TPA peaks may be the result of different transition characters. The results also show that OPA spectra of all the studied molecules are located in the UV range. In conclusion, investigated Pt-acetylides (**1**, **2**, **3**, and **PE2**) are demonstrated to be good two-photon absorption materials exhibiting, at the same time, strong two-photon absorption and good transparency for OPL applications.

Acknowledgment. This work is supported by the National Natural Science Foundation of China and the State Key Laboratory for Supramolecular Structure and Material of Jilin University.

Supporting Information Available: Geometric parameters of **1-trans** and **2-trans** (Table 1); contour surfaces of the frontier orbitals relevant to the maximal two-photon absorptions for **1-cis**, **2-cis**, and **3-cis** (Figure 1); ZINDO predicted transition dipole moments between main electronic states (Figure 2); and Cartesian coordinates of all studied molecules. This material is available free of charge via the Internet at http://pubs.acs.org.

IC800417G